Beyond Weather Time-Scale Prediction for Hurricane Sandy and Super Typhoon Haiyan in a Global Climate Model

BAOQIANG XIANG,* SHIAN-JIANN LIN,+ MING ZHAO,* SHAOQING ZHANG,+ GABRIEL VECCHI,+ TIM LI,# XIANAN JIANG,@ LUCAS HARRIS,+ AND JAN-HUEY CHEN*

* *NOAA/Geophysical Fluid Dynamics Laboratory, Princeton, New Jersey, and University Corporation for Atmospheric Research, Boulder, Colorado*
+ *NOAA/Geophysical Fluid Dynamics Laboratory, Princeton, New Jersey*
# *International Pacific Research Center, Department of Meteorology, University of Hawai'i at Mānoa, Honolulu, Hawaii*
@ *Joint Institute for Regional Earth System Science and Engineering, University of California, Los Angeles, Los Angeles, California*

(Manuscript received 13 July 2014, in final form 27 August 2014)

ABSTRACT

While tropical cyclone (TC) prediction, in particular TC genesis, remains very challenging, accurate prediction of TCs is critical for timely preparedness and mitigation. Using a new version of the Geophysical Fluid Dynamics Laboratory (GFDL) coupled model, the authors studied the predictability of two destructive landfall TCs: Hurricane Sandy in 2012 and Super Typhoon Haiyan in 2013. Results demonstrate that the geneses of these two TCs are highly predictable with the maximum prediction lead time reaching 11 days. The ''beyond weather time scale'' predictability of tropical cyclogenesis is primarily attributed to the model's skillful prediction of the intraseasonal Madden–Julian oscillation (MJO) and the westward propagation of easterly waves. Meanwhile, the landfall location and time can be predicted one week ahead for Sandy's U.S landfall, and two weeks ahead for Haiyan's landing in the Philippines. The success in predicting Sandy and Haiyan, together with low false alarms, indicates the potential of using the GFDL coupled model for extended-range predictions of TCs.

1. Introduction

Tropical cyclones (TCs) are one of the most common and devastating natural disasters that result in serious impacts on marine activities and coastal communities. Two intense landfall TCs—Sandy in 2012 and Haiyan in 2013—have received great attention given their severe damages and the resultant enormous losses (Blake et al. 2013; Malakoff 2012; Lander et al. 2014).

On 21 October 2012, the storm that would become Hurricane Sandy formed over the central Caribbean. The incipient Sandy moved northward over Jamaica on 24 October, over Cuba the following day, and continued migrating northward thereafter. After passing near Bermuda, Sandy curved northwestward and made landfall along the densely populated U.S. Atlantic coast near Atlantic City, New Jersey, late on Monday evening, 29 October. Sandy was the second most expensive Atlantic TC in history, causing over $60 billion (U.S. dollars) in damage, and claimed 147 lives in Jamaica, Cuba, Haiti, the Dominican Republic, Puerto Rico, the Bahamas, the United States, and Canada (Blake et al. 2013). Sandy was the largest Atlantic TC since those records began on 1988, causing wind damage as far inland as the Indiana shore of Lake Michigan (Blake et al. 2013). Despite its impact and size, Sandy was only a minimal category 1 hurricane upon landfall and had been undergoing extratropical transition into a midlatitude cyclone.

Much more intense, and much deadlier, was Super Typhoon Haiyan, which occurred just over a year after Sandy. Haiyan formed in the western North Pacific (WNP) on 3 November 2013, and a few days later underwent a rapid intensification. It first affected the Federated States of Micronesia and Palau. Satellite estimates indicated a storm with 1-min sustained winds possibly as

Corresponding author address: Baoqiang Xiang, GFDL, UCAR, 201 Forrestal Rd., Princeton, NJ 08540.
E-mail: baoqiang.xiang@noaa.gov

DOI: 10.1175/MWR-D-14-00227.1

high as 87.5 m s^{-1} on 7 November (Lander et al. 2014), before making a cataclysmic landfall near Guiuan, eastern Samar. Haiyan then crossed the Philippines, migrated westward into the South China Sea, and made its landfall in Vietnam as a weak TC. This storm caused more than 6000 deaths and left 14 million affected. (http://reliefweb.int/sites/reliefweb.int/files/resources/HB-AP-2013.FINAL__0.pdf) Typhoon Haiyan reached a category 5–equivalent super typhoon on the Saffir–Simpson hurricane wind scale as the strongest TC in 2013 and also the strongest TC at landfall on world record (Lander et al. 2014).

Previous studies have primarily focused on track predictions only after tropical cyclogenesis has occurred, and prediction skill has been steadily increasing in recent decades. For example, the Atlantic basin TC track error has been reduced substantially from around 400 km in the 1970s to around 100 km in the early 2010s with respect to the 3-day lead forecast (http://www.nhc.noaa.gov/verification/verify5.shtml). For Hurricane Sandy, the European Centre for Medium-Range Weather Forecasts (ECMWF) made a successful prediction of the TC ashore one week ahead (Kerr 2012). The U.S. models in general showed less skill in predicting the landfall for Sandy than the ECMWF model (Blake et al. 2013).

Our knowledge about cyclogenesis is severely limited in understanding whether an observational tropical disturbance will evolve into a full TC or not although some progresses have been achieved recently (e.g., Fu et al. 2012; Peng et al. 2012). Thus, cyclogenesis prediction is still a challenging task that remains an area requiring considerable additional research. Up to now, the Joint Typhoon Warning Center (JTWC) only provides 24-h TC genesis forecast for the western Pacific and Indian Oceans, and the National Hurricane Center (NHC) provides 48-h and 5-day experimental TC genesis probability forecast for other basins including the Atlantic and eastern Pacific.

Geophysical Fluid Dynamics Laboratory (GFDL) global climate models have been used for seasonal forecast for TC genesis with significant prediction skill (Chen and Lin 2013; Vecchi et al. 2014), while its capability in predicting an individual TC has not been studied yet. In this study, a new version of the GFDL coupled model is used to explore the predictability of individual TC (Sandy and Haiyan), and demonstrate the potential of this model for extended-range TC prediction.

2. Data, model, and methodology

The observational TC data before 2013 are from the International Best Track Archive for Climate Stewardship (IBTrACS) version v03r05 (Knapp et al. 2010), and given the data lag for incorporating 2013 seasonal data into IBTrACS, the track data for Typhoon Haiyan are obtained directly from the Regional Specialized Meteorological Center in Tokyo (http://www.jma.go.jp/jma/jma-eng/jma-center/rsmc-hp-pub-eg/trackarchives.html). For comparison with Sandy-induced precipitation and snowfall, we use the observed daily rainfall databased on the Tropical Rainfall Measuring Mission (TRMM) version 3B42 (Huffman et al. 1995), and daily snowfall analysis data from the National Operational Hydrologic Remote Sensing Center.

A new version of GFDL coupled model was employed in this study, which is similar to the Forecast-Oriented Low Ocean Resolution (FLOR) version (Vecchi et al. 2014) of GFDL CM2.5 (Delworth et al. 2012). The main difference between the new model and FLOR is the convection scheme in the atmospheric model. Based on the GFDL High Resolution Atmospheric Model (HiRAM) with a single convective plume (Zhao et al. 2009), the new convection scheme introduces an additional bulk plume to represent deep convection [referred to as a double-plume convection (DPC) scheme]. More details about the convection scheme and its performance in climate simulations are referred to in M. Zhao et al. (2015, unpublished manuscript). The ocean model horizontal resolution is about 1°, and the atmospheric model has a roughly 50-km horizontal grid spacing and 32 vertical levels, formulated on a ''cubed sphere'' grid described on 6 sides of a cube projected onto a sphere (Putman and Lin 2007).

The initial conditions are obtained through a simple nudging method. The atmospheric nudging fields include winds, surface pressure, geopotential height, and temperature using the National Centers for Environmental Prediction (NCEP) Global Forecast System (GFS) analysis data (~28 km, 6-h interval) as used in Chen and Lin (2013) for seasonal hurricane predictions. Following Zhang et al. (2014), the sea surface temperature (SST) is nudged to National Oceanic and Atmospheric Administration (NOAA) Optimum Interpolation ¼ Degree Daily SST Analysis (OISST, v2) (Reynolds et al. 2007). The nudging time scale is 6 h for atmospheric variables and 1 day for SST. The coupled model is spun up with the observed atmospheric and SST conditions from 1 January 2010 to October 2012 and October 2013 to generate the initial conditions for predicting Sandy and Haiyan. Initial conditions are archived each hour. Each ensemble is integrated forward one month for prediction.

A simple tracking scheme is adopted using primarily the sea level pressure (SLP) to detect TCs (L. Harris et al. 2015, unpublished manuscript). We have compared the results by using another tracking

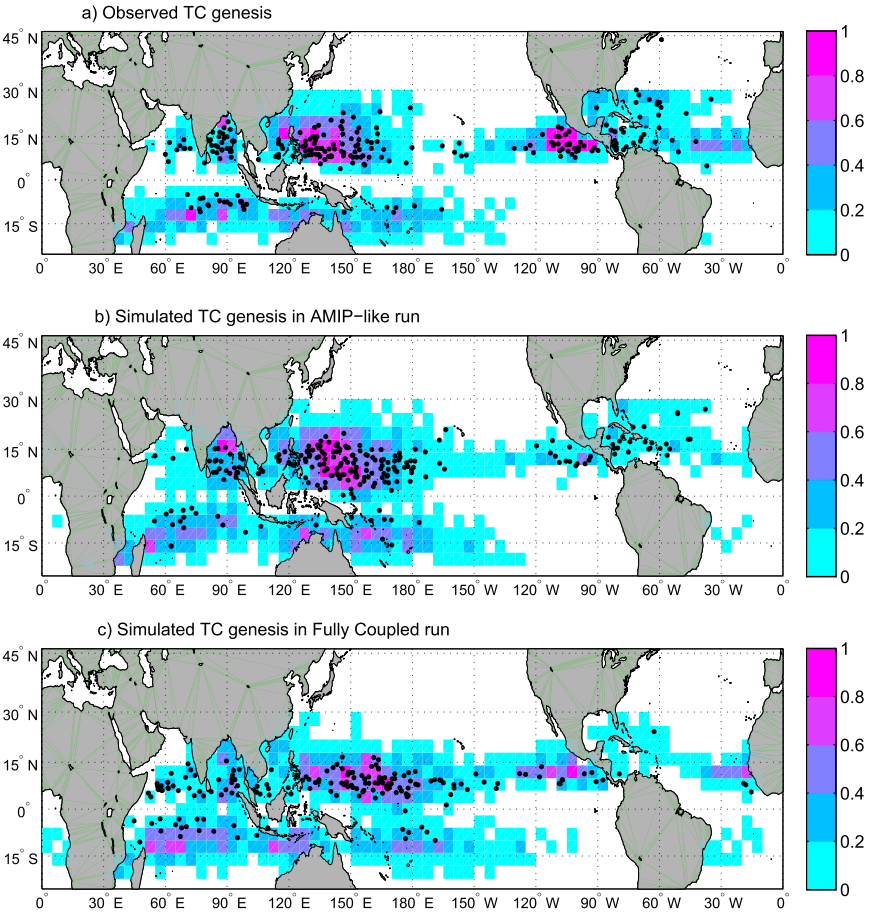

FIG. 1. Annual tropical cyclogenesis density (shading in number per year) in (a) observations (1983–2012), (b) AMIP-like runs with daily SST nudging forcing, and (c) fully coupled runs. Cyclogenesis is defined as the mean number per 5° (longitude) × 4° (latitude) box per year. The black dots show the genesis location during 15 Oct to 14 Nov when Tropical Cyclones Sandy and Haiyan formed. A total of 30 years of data are used here. Here only the tropical cyclones with lifetimes of at least 3 days are shown.

scheme (Zhao et al. 2009) and the results remain very similar.

3. Results

a. Climatological tropical cyclogenesis in the model

Before examining model prediction skill for Sandy and Haiyan, it is informative to investigate the model's general performance in simulating climatological tropical cyclogenesis especially during the latter portion of TC season. Figure 1 depicts the climatology of tropical cyclogenesis for a 30-yr period from observations, an Atmospheric Model Intercomparison Project (AMIP)-like simulation, and a fully coupled simulation. Here the "AMIP-like" simulation is referred to a coupled run but with daily SST nudging to observations from 1984 to 2013. In general, the genesis location and density agree reasonably well with observations in both of these experiments. The annual mean TC counts in AMIP-like and fully coupled runs are 80.8 and 79.8, respectively, in great agreement with the observed value of 81.1 per year. Note that the TCs with lifetimes less than 3 days were excluded. The most apparent bias is more cyclogenesis over the Eastern Hemisphere but less over the Western Hemisphere (Fig. 1). In the fully coupled run, considerable bias is seen over the WNP with the maximum center expanding far more eastward (Fig. 1c). Additionally, compared with both the observations and AMIP-like run, the genesis density is lower over the western North Atlantic but more over the southern Atlantic in the coupled simulation.

Since Hurricane Sandy and Super Typhoon Haiyan were generated during the latter portion of their TC seasons, special attention was paid to the period from 15 October to 14 November (black dots in Fig. 1). It is noted that the coupled run produces very few TCs

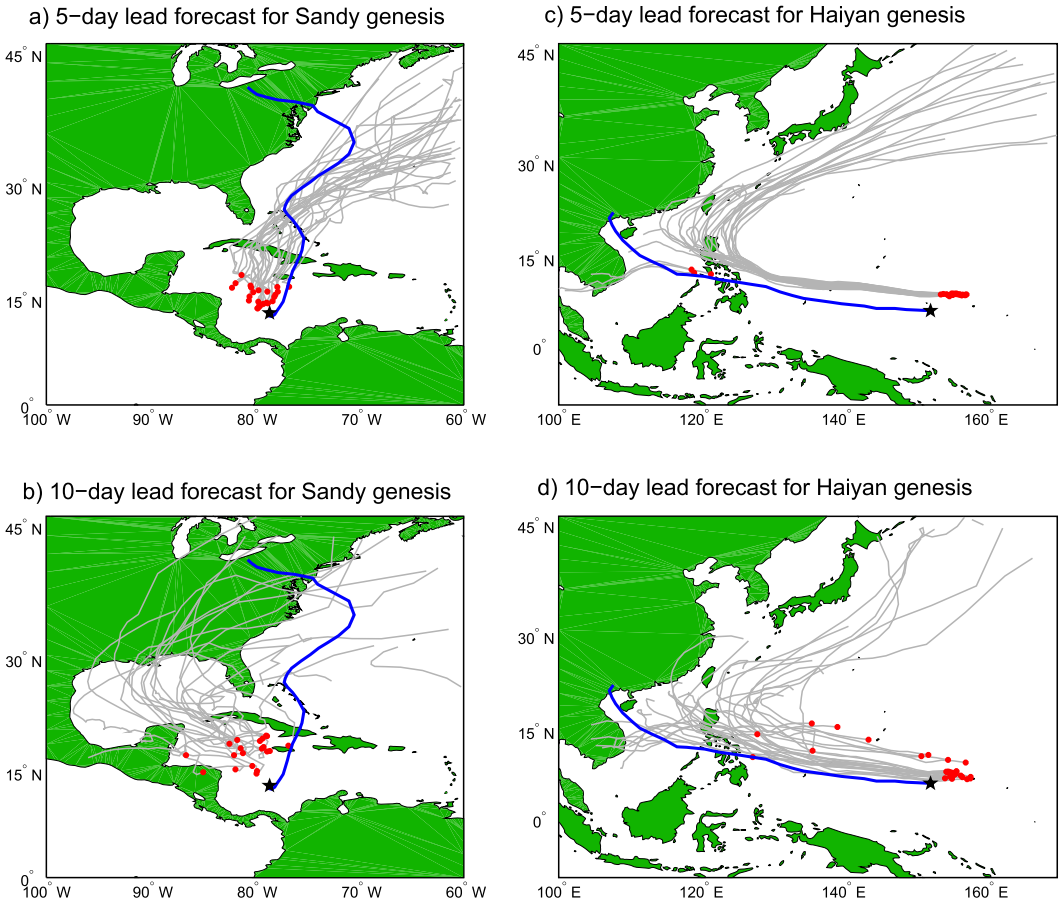

FIG. 2. The 5- and 10-day lead forecasts for the geneses of Sandy and Haiyan with 25 ensemble members for each daily prediction. Blue (gray) lines represent the observed (predicted) TC track. Black stars (red dots) show the observed (predicted) genesis locations.

over the Caribbean Sea within 30 years (Fig. 1c), while this is much improved in the AMIP-like run despite the northward displacement of genesis location (black dots in Fig. 1b). Over the WNP, both the fully coupled and AMIP-type runs produced more TCs to the east of 170°E. However, less TC genesis is evident over the region west of 140°E. As expected, the AMIP-type run performs better in simulating cyclogenesis because of the better mean state, which justifies the mean state (SST) adjustment for seasonal prediction (Vecchi et al. 2014). For the short-term prediction, however, the SST nudging would be suitable as the mean state is not expected to drift much from the initial conditions.

b. *Cyclogenesis prediction*

The above results illustrate the capability of the GFDL model in simulating the climatology of tropical cyclogenesis. Given this, a series of hindcast experiments are made for both Sandy and Haiyan. Figure 2 depicts the 5- and 10-day lead forecast results, where 25 members are used for each day. For example, the cyclogenesis time for Sandy (when it became a tropical storm) was found at 1200 UTC 22 October 2012. For the 5-day lead forecast the initial conditions for these 25 ensemble members were produced with the coupled system nudging from 0000 UTC 17 October to 0000 UTC 18 October (one forecast every hour). The "correct" prediction is counted by the cyclogenesis within 1.5 days around the observed genesis time (a 3-day window). Here, we define cyclogenesis as the time when the cyclone reaches tropical storm status [with winds $>17.5\,\mathrm{m\,s^{-1}}$ in observations and $15.2\,\mathrm{m\,s^{-1}}$ in the model following Zhao et al. (2009)] rather than tropical depression because the time at which the tropical depression forms varies considerably among ensemble members. In other words, more TCs formed beyond the correct time window if the genesis time is defined as the TC first reaching tropical depression. However, the conclusions will not change since the time difference for

a disturbance becoming a tropical depression compared to a tropical storm is usually within one day of each other.

Figure 2 shows that most of the members produce "Sandy like" and "Haiyan like" TCs with their genesis locations slightly to the north or northeast of the observations for both the 5- and 10-day lead forecasts. The location biases to a certain degree reflect the systematic bias of the model as shown in Fig. 1. The genesis locations are rather concentrated for different ensemble members, indicative of the high predictability of cyclogenesis for these two cases.

To quantitatively measure the cyclogenesis prediction skill, a traditional verification statistics, namely, probability of detection (POD, or named hit rate) is used here. As mentioned above, we use a correct prediction time window, 1.5 days around the observed genesis time. We use spatial limits of 600, 700, and 800 km for 5-, 6-, and 7-day lead forecasts, respectively, and 900 km for 8- to 13-day lead forecasts. Meanwhile, the early and late genesis cases are defined as the cyclone numbers 1.5 days before and 1.5 days after the correct prediction time window, but with the same spatial limits as the correct forecasts. For example, for the 5-day lead forecast, 25 ensemble members predict 12 cases during the 3-day correct forecast window, and 8 cases during 1.5 days before and after the correct forecast window. Thus, the POD is 48.0% (12/25), and the early/late genesis ratio is 32.0% (8/25). From the 5- to 11-day lead forecast, the POD is all above 60% for both Sandy and Haiyan (Fig. 3). The skill drops dramatically for the 12- and 13-day lead forecasts. Meanwhile, there are some early/late genesis cases for Sandy for the 7–13-day lead forecasts, implying that the model still has some skill in predicting the Sandy genesis for the 12- and 13-day lead forecasts. In contrast, there are only a few early/late genesis cases for Haiyan for the 10- and 11-day lead forecasts. The above results suggest that the geneses of these two TCs are highly predictable for a lead time of at least 11 days, a time scale slightly beyond the medium-range weather time scale (~7–10 days).

During 21–23 October 2012, there were four TCs worldwide including Sandy that provided additional opportunities to test the validity of our methodology and model performance (Fig. 4). In addition to Sandy, the geneses of the other three TCs are also skillfully predicted with at least a 6-day lead time, and this included a weak TC over the Arabian Sea that can even be predicted 10 days in advance (not shown). Intriguingly, the model produces very few false alarms spatially (Figs. 4a,b), which is another crucial aspect in measuring the skill of TC prediction. These results suggest the great potential

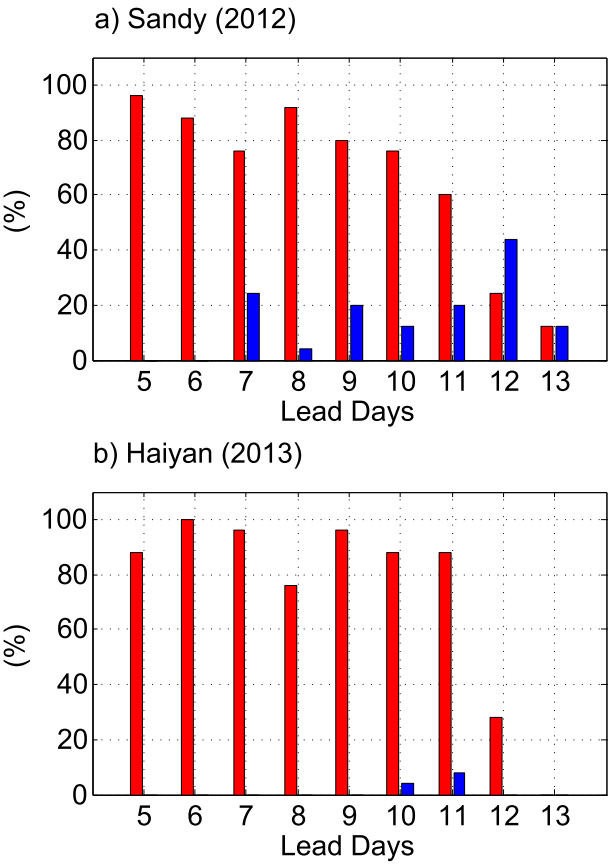

FIG. 3. Measure of prediction skill for (a) Sandy and (b) Haiyan. Red and blue bars represent the probability of detection (POD) and early/late genesis ratio, respectively. A total of 25 members are used for each daily prediction.

of our model in predicting the tropical cyclogenesis during the latter TC season.

c. *Understanding the predictability source of cyclogenesis*

The U.S. National Weather Service issues medium-range weather forecasts over the next 3–7 days and extended-range forecasts for 6–10 and 8–14 days. By contrast, the definition of medium-range forecasts from the World Meteorological Organization (WMO) is 7–10 days, and 10 days up to 1 month for extended-range forecasts. The beyond weather (or extended range) time scale is usually thought to be a difficult time range for prediction, as it is sufficiently long for the atmosphere to lose its memory from initial condition and probably too short for oceanic variability to provide a predictability source (Vitart 2014). However, some low-frequency variability modes in the atmosphere–ocean coupled system may provide a predictability source for cyclogenesis, such as the intraseasonal Madden–Julian oscillation (MJO; Fudeyasu et al. 2008; Fu and Hsu 2011;

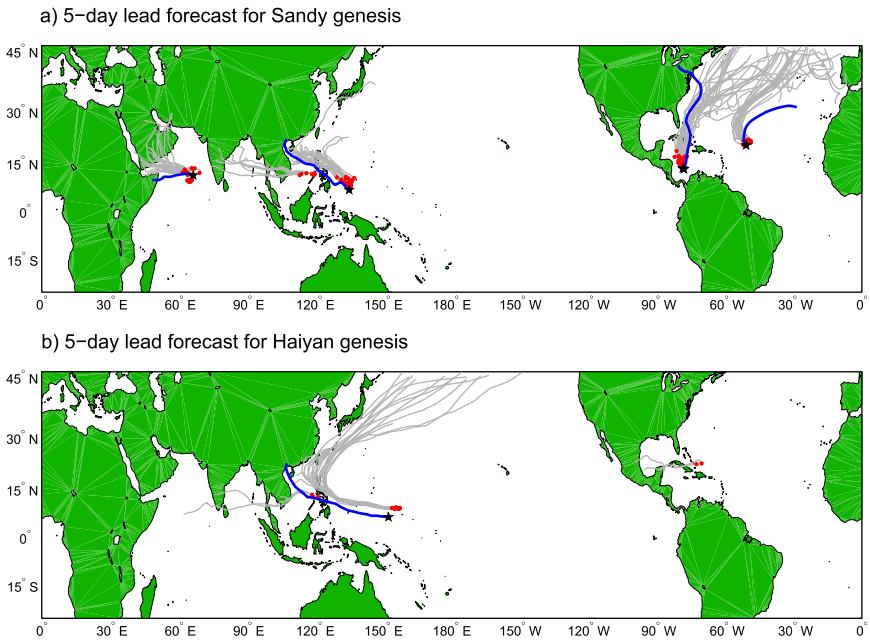

FIG. 4. The 5-day lead prediction for the geneses of (a) Sandy and (b) Haiyan. Blue and gray lines show the track for observation and prediction, respectively. Black stars (red dots) represent the observed (predicted) tropical cyclogenesis locations.

Vitart 2009, 2010; Belanger et al. 2010; Elsberry et al. 2010), tropical waves (Frank and Roundy 2006), and persistent SST anomaly (Leroy and Wheeler 2008).

As the most dominant intraseasonal mode over the tropics, MJO has long been revealed to have a tight relationship with cyclogenesis (Liebmann et al. 1994; Maloney and Hartmann 2000; Mo 2000; Camargo et al. 2009; Jiang et al. 2012; Diamond and Renwick 2014). The extended-range TC predictability might be conceived in the skillful prediction of MJO. We examined the MJO signals before the Sandy and Haiyan genesis by using a 20–100-day bandpass-filtered data for observations and 7-day running mean data for model prediction (after removing its 1-month mean). As shown in Fig. 5a, before Sandy genesis, strong intraseasonal westerly wind prevailed over the northeastern Pacific and south Caribbean Sea accompanying pronounced precipitation mainly over the Caribbean Sea, representing a typical active phase of MJO over this region (Maloney and Hartmann 2000). Before Haiyan genesis, enhanced precipitation was apparent over the WNP but suppressed precipitation was over the Maritime Continent and the north Indian Ocean (Fig. 5c), suggesting a typical phase 5 of boreal summer MJO mode (Waliser et al. 2009). How does MJO influence the cyclogenesis? Increased low-level absolute vorticity and the moistening of the midtroposphere due to enhanced surface heat flux and convection, were argued to facilitate the cyclogenesis (Maloney and Hartmann 2000; Camargo et al. 2009). One distinct difference between these two cases is that the pronounced lower-level convergence is apparent over the WNP (around 150°E), but not over the Caribbean Sea (Fig. 5). The presence of the large-scale confluent flow associated with MJO in the WNP may favor the energy accumulation of easterly waves as well as the formation of TCs (Tam and Li 2006). The model predicts well the low-level wind and precipitation prior to the Sandy and Haiyan genesis (Figs. 5b and 5d), suggesting that the skillful prediction of MJO may play a prominent role on the successful predictions of Sandy and Haiyan.

Yet, it should also be noted that the MJO usually exhibits a larger spatial scale and longer time scale than TCs. A successful prediction of an active phase of the MJO provides a wide time window and a large spatial area favoring the tropical cyclogenesis. However, our model prediction illustrated that the predicted genesis timing was in a narrow time window, and the locations were rather concentrated and close to the observed genesis location for the majority of the predicted cyclogenesis (Fig. 2). This indicates that some other factors may work cooperatively for skillful prediction of cyclogenesis. Although there are substantial differences for the precursor disturbance between the Atlantic and WNP, easterly waves act as one common factor triggering the TC development in these two basins (e.g., Landsea 1993; Ritchie and Holland 1999; Belanger et al. 2010; Li 2012). The TC genesis associated with easterly waves usually tends to occur near the intersection of the

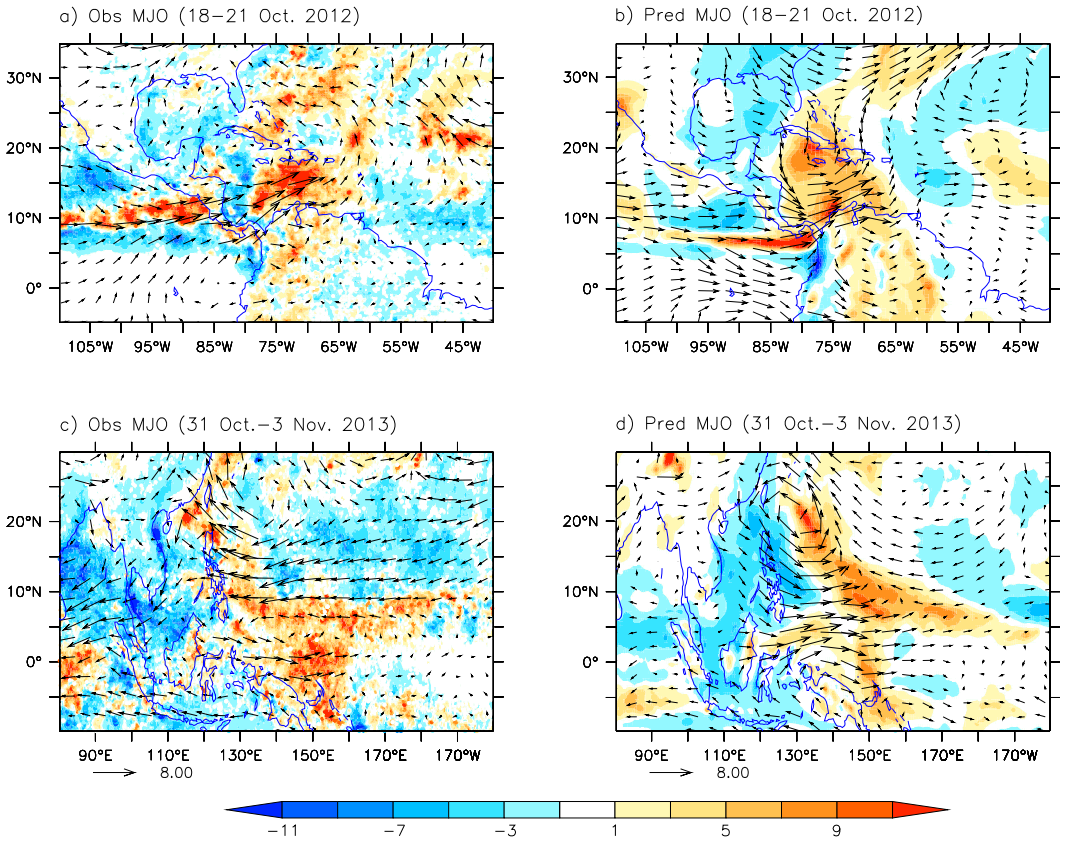

FIG. 5. Observed and predicted MJO signals before Sandy and Haiyan genesis. (a) The 20–100-day filtered precipitation (shading, mm day^{-1}) and 850-hPa winds (vectors, m s^{-1}) averaged over 18–21 Oct 2012. Precipitation is from TRMM data and winds are from NCEP analysis data. (b) Predicted MJO signal during 18–21 Oct 2012 for 10-day lead forecast for Sandy genesis with initial condition roughly on 12 Oct 2012. For model prediction, the MJO signal is obtained by using 5-day running mean after removing the corresponding 1-month mean in prediction. (c),(d) As in (a),(b), but for Haiyan prediction (31 Oct–3 Nov 2013).

critical surface and the trough axis of the precursor parent wave according to the so-called marsupial theory (Dunkerton et al. 2009; Wang et al. 2009). The westward propagation of easterly waves offers predictability for the TC genesis. The 3–8-day bandpass-filtered 700-hPa meridional wind averaged over 5°–17° clearly features the easterly wave couplets starting from the west coast of Africa on around 11 October 2012 and propagating westward into the Caribbean Sea (Fig. 6a). The 10-day lead forecast can reasonably predict the propagation of easterly waves (Fig. 6c), leading to the genesis of "Sandy" after reaching the convective center related to MJO (Fig. 5a). Similarly, the external forcing from a train of Pacific easterly waves, manifested as wave couplets in the 850-hPa meridional wind, was also crucial in triggering the Haiyan's genesis although the predicted easterly waves were weaker than what was observed (Figs. 6b,d). The Pacific easterly waves propagate into the convective region associated with MJO (west of 170°E) and stall for about two days before a TC formed. Along the easterly wave track, another reason for the genesis location in the Caribbean Sea and WNP (near 150°E) rather than in their eastern part is the relatively stronger mean vertical wind shear and cooler SST in the eastern Atlantic and eastern Pacific.

Here we did not emphasize the possible role of SST for the geneses of these two TCs based on the following reasons. Before Sandy's genesis, about 0.2°C SST warming was found over the south Caribbean Sea. This is due to the MJO variability as the anomalous intraseasonal westerly wind (Fig. 5a) is against the climatological mean easterly wind so as to reduce the mean evaporation. From late June of 2013, pronounced SST warming (>0.3°C) was seen over the western Pacific including the region of Haiyan's genesis. It lasted for several months and thus should be excluded as the direct factor driving the Haiyan genesis.

d. Trajectory and landfall prediction

For Typhoon Haiyan, the model predicted a reasonable westward trajectory in forecasts initialized at both 5

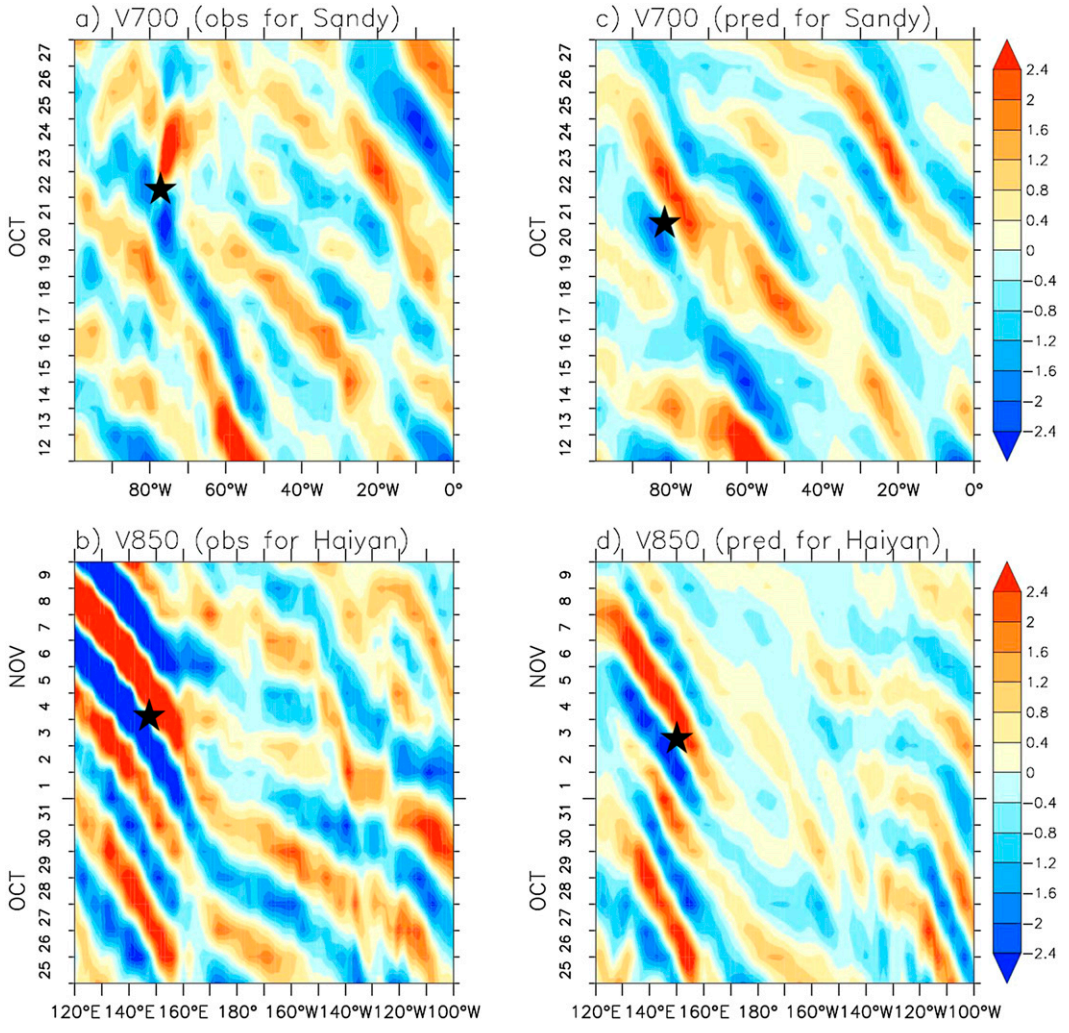

FIG. 6. Observed and predicted easterly waves for Sandy and Haiyan. The 700-hPa meridional winds (5°–17°N) from (a) observations and (c) ensemble mean of model prediction on 12 Oct 2012. The 850-hPa meridional winds (5°–10°N) from (b) observations and (d) ensemble mean of model prediction on 25 Oct 2013. Black stars show the approximate cyclogenesis. Here a 3–8-day bandpass filter is applied to the wind data, while for prediction, the observed data are used before the prediction starting time. A wave propagation feature is more apparent at 850 hPa than that at 700 hPa for Haiyan (not shown).

and 10 days prior to its genesis despite a systematic northward bias (Fig. 2). Meanwhile, most of the ensemble members show the landfall time in Samar, Philippines, on 7 November 2013 for both 5- and 10-day lead forecasts, implying that the model has the capability to predict its first landfall with a lead time of about two weeks. For Hurricane Sandy, the 5-day lead forecast predicted a reasonable northward movement crossing Cuba as a typical storm trajectory in the latter TC season over this region, but failed to predict its northwestward curvature toward the northeastern United States. The 10-day lead forecast exhibited a diverse track with most of the ensemble members predicting a westward trajectory to the Gulf of Mexico, suggesting that the model completely loses all skill in predicting the actual trajectory.

The predicted northwestward curvature of Sandy in the midlatitudes continues to pose a great forecasting challenge. With the initial conditions before the observed genesis, this model was not able to predict this northwestward turn as well as the final landfall into the United States. However, the successful prediction can be achieved with initial condition on 22 October 2012 after its genesis despite the slightly northward landfall location (Fig. 7a). The atmospheric nudging is applied beyond a radius of 300 km and we use a ''bogus'' method to incorporate the observational SLP associated with Sandy (from IBTrACS) into the 300-km radius area

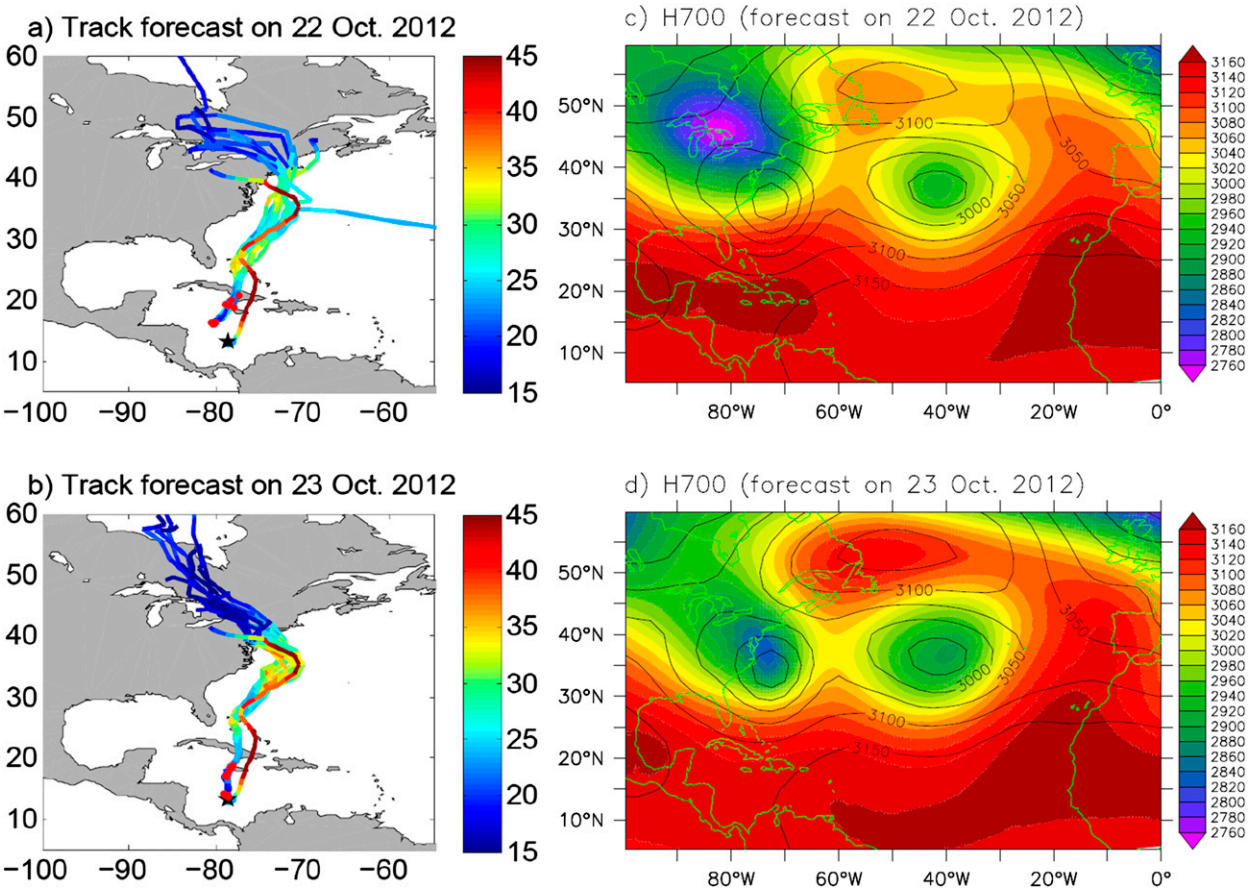

FIG. 7. Track forecast of Sandy on (a) 22 Oct and (b) 23 Oct 2012. A total of 12 ensemble members are used here. The observational Sandy genesis is marked by black star. (c),(d) The corresponding 700-hPa geopotential height from observations (contours) and model prediction (shading) during 28–29 Oct 2012 when Sandy made its landfall.

near the TC center before the real forecast. The reason we did not use the NCEP analysis data nudging near the TC center is due to the fact that the assimilation of atmospheric data tends to filter out small-scale perturbations, prohibiting the potential development of TCs in the model (Zhang et al. 2014). The bogus method is only suggested to use for prediction after TC genesis. With the initial condition on 23 October, almost all the members are capable of predicting its landfall location on New Jersey (Fig. 7b) as well as the landfall time on late 29 October or early 30 October. The northwestward curvature is mainly driven by a high pressure system over the northwestern Atlantic Ocean (Barnes et al. 2013). The model can well predict this high center near 55°N, 50°W (Figs. 7c,d), leading to the successful landfall prediction for Sandy. The track prediction skill is comparable with the ECMWF forecast results (Kerr 2012). The anomalous high in the North Atlantic actually reflects one component of a strong negative phase of North Atlantic Oscillation (NAO). Further analysis shows that the NAO-related winds largely stems from the 20–100-day intraseasonal variability (ISV). It gives a clue that the predictability source for the landfall of Sandy may also come from the ISV, which may also be linked to the tropical MJO-forcing effect (Cassou 2008).

While the landfall location for Sandy was in New Jersey, the maximum precipitation associated with Hurricane Sandy and its extratropical remnants were observed near southern Maryland and Delaware for 27–31 October 2012 (Blake et al. 2013). The predicted precipitation pattern is very similar to observations with a maximum over 200 mm (8 in.) (Fig. 8b). Of particular interest is that the model does very well in predicting the pattern of the tropical cyclone–induced snowfall that occurred over West Virginia and Pennsylvania but with underestimated amplitude (Fig. 8d). We also examine the precipitation associated with Haiyan, and the model can predict the precipitation reasonably well with two weeks lead time, although the maximum center shifts northward together with weakened magnitude (Figs. 8e,f). These results are encouraging.

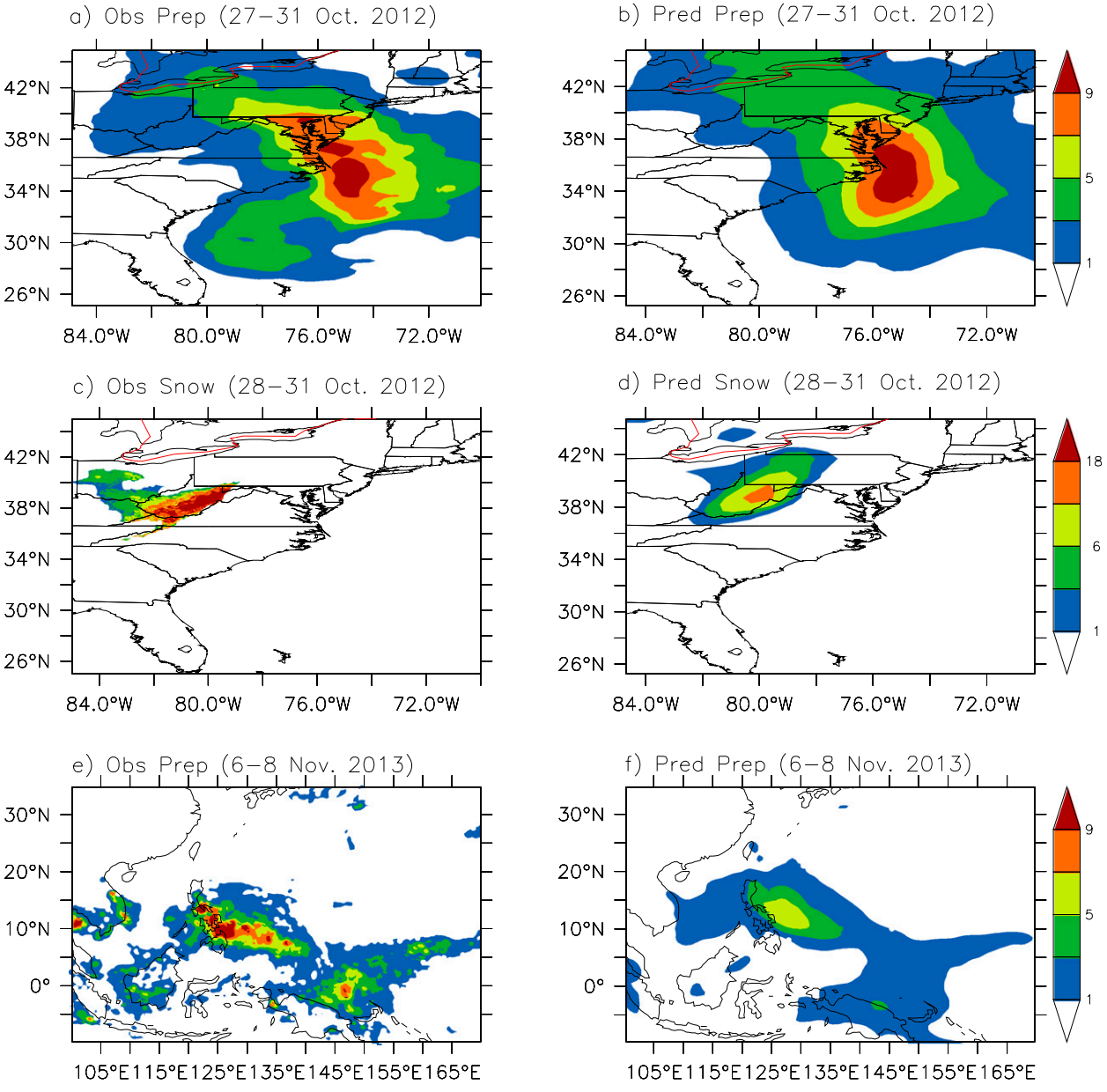

FIG. 8. (a) Observed (five gridpoint smoothed) and (b) predicted precipitation (in.) associated with Hurricane Sandy and its extratropical remnants during 27–31 Oct 2012, with initial condition on 23 Oct 2012. (c),(d) As in (a),(b), but for snowfall (in.) during 28–31 Oct 2012. (e) Observed and (f) predicted precipitation (in.) associated with Super Typhoon Haiyan during 6–8 Nov 2013 with an initial condition on 25 Oct 2013.

4. Conclusions and discussion

The Superstorm Sandy in 2012 was the largest TC (by area) over the Atlantic basin on record and Haiyan in 2013 was the strongest landfall typhoon in history. Understanding the predictability of their genesis has great societal and scientific significance. This study attempts to reveal the predictability of these two TCs by using a new version of the GFDL coupled model system with a simple atmospheric and SST nudging method for initialization. Results show that the geneses of both TCs can be well predicted with a lead time of 11 days, a skill beyond the medium-range of weather forecasts. Further analysis suggests that these two TCs share a similar source of predictability for genesis, which is attributed to the MJO and the westward propagation of easterly waves. The landfalls of Sandy and Haiyan can also be well predicted with one- and two-week lead times, respectively. Although this study focused only on two important cases, it may give us some confidence using this model for individual TC

prediction, especially for those triggered by the MJO and easterly waves. This study suggests some potential improvements of the lead time of current operational forecasts and provides useful guidance on extended-range time-scale TC forecasts, while a larger, statistical sample size is needed to thoroughly evaluate this model.

A sensitivity test for the impacts of model physics on TC predictive skills was also performed. The GFDL HiRAM atmospheric model has been demonstrated to be one of the best models in simulating and predicting TCs especially over the Atlantic Ocean when forced by observed SST (Chen and Lin 2013; Zhao et al. 2009; Shaevitz et al. 2014). Forecasts were also carried out by using the coupled model but with the HiRAM atmospheric model component (retaining exactly the same for other components and the initialization). The 5-day lead forecast has no skill (no ensemble members predicting the Sandy-like TC) in predicting the geneses of Sandy mainly because of the unrealistically strong vertical wind shear over the Caribbean Sea in the predictions (figure not shown). The improved skill in TC prediction may be attributed to a better representation of the tropical mean state through adoption of the new DPC cumulus scheme over the single plume convective scheme as used in HiRAM.

It should be noted that here we use a relatively coarse-resolution atmospheric model (~50 km) for TC prediction and a very simple initialization method (nudging) compared to operational forecast systems. Thus, our forecast experiments show very encouraging results and suggest large potential for future operational forecasts. Given the skillful predictions skill on seasonal to decadal time scales of GFDL coupled models (e.g., Vecchi et al. 2014; Jia et al. 2015; Yang et al. 2013), we have increased confidence to develop and deliver a seamless forecast model from weather to climate time scales. A more comprehensive assessment of the predictability of cyclogenesis and TC track will be conducted based on forecasts of more TC events in the future.

Acknowledgments. The authors appreciate helpful comments from Howard Diamond and they benefitted from the discussions with Frederic Vitart, Zhuo Wang, Xiaosong Yang, and Hiroyuki Murakami. The authors acknowledge support from NOAA under Grant NA14OAR4830101 (BX, SJL, GV, and JHC) and NOAA MAPP Program under Awards NA12OAR4310075 (BX, MZ, XJ). TL was supported by ONR Grant N00014-12-10450.

REFERENCES

Barnes, E. A., L. M. Polvani, and A. H. Sobel, 2013: Model projections of atmospheric steering of Sandy-like superstorms. *Proc. Natl. Acad. Sci.,* **110,** 15 211–15 215, doi:10.1073/pnas.1308732110.

Belanger, J. I., J. A. Curry, and P. J. Webster, 2010: Predictability of North Atlantic tropical cyclone activity on intraseasonal time scales. *Mon. Wea. Rev.,* **138,** 4362–4374, doi:10.1175/2010MWR3460.1.

——, P. J. Webster, J. A. Curry, and M. T. Jelinek, 2012: Extended prediction of North Indian Ocean tropical cyclones. *Wea. Forecasting,* **27,** 757–769, doi:10.1175/WAF-D-11-00083.1.

Blake, E. S., T. B. Kimberlain, R. J. Berg, J. P. Cangialosi, and J. L. Beven III, 2013: Tropical cyclone report: Hurricane Sandy (AL182012) 22–29 October 2012. Tech. Rep. AL182012, NOAA/National Hurricane Center, 157 pp. [Available online at http://www.nhc.noaa.gov/data/tcr/AL182012_Sandy.pdf.]

Camargo, S. J., M. C. Wheeler, and A. H. Sobel, 2009: Diagnosis of the MJO modulation of tropical cyclogenesis using an empirical index. *J. Atmos. Sci.,* **66,** 3061–3074, doi:10.1175/2009JAS3101.1.

Cassou, C., 2008: Intraseasonal interaction between the Madden-Julian Oscillation and the North Atlantic Oscillation. *Nature,* **455,** 523–527, doi:10.1038/nature07286.

Chen, J.-H., and S.-J. Lin, 2013: Seasonal predictions of tropical cyclones using a 25-km-resolution general circulation model. *J. Climate,* **26,** 380–398, doi:10.1175/JCLI-D-12-00061.1.

Delworth, T. L., and Coauthors, 2012: Simulated climate and climate change in the GFDL CM2.5 high-resolution coupled climate model. *J. Climate,* **25,** 2755–2781, doi:10.1175/JCLI-D-11-00316.1.

Diamond, H. J., and J. A. Renwick, 2014: The climatological relationship between tropical cyclones in the southwest Pacific and the Madden–Julian Oscillation. *Int. J. Climatol.,* doi:10.1002/joc.4012, in press.

Dunkerton, T. J., M. T. Montgomery, and Z. Wang, 2009: Tropical cyclogenesis in a tropical wave critical layer: Easterly waves. *Atmos. Chem. Phys.,* **9,** 5587–5646, doi:10.5194/acp-9-5587-2009.

Elsberry, R. L., M. S. Jordan, and F. Vitart, 2010: Predictability of tropical cyclone events on intraseasonal timescales with the ECMWF monthly forecast model. *Asia-Pac. J. Atmos. Sci.,* **46,** 135–153, doi:10.1007/s13143-010-0013-4.

Frank, W. M., and P. E. Roundy, 2006: The relationship between tropical waves and tropical cyclogenesis. *Mon. Wea. Rev.,* **134,** 2397–2417, doi:10.1175/MWR3204.1.

Fu, B., M. S. Peng, T. Li, and D. E. Stevens, 2012: Developing versus nondeveloping disturbances for tropical cyclone formation. Part II: Western North Pacific. *Mon. Wea. Rev.,* **140,** 1067–1080, doi:10.1175/2011MWR3618.1.

Fu, X., and P. Hsu, 2011: Extended-range ensemble forecasting of tropical cyclogenesis in the northern Indian Ocean: Modulation of Madden-Julian Oscillation. *Geophys. Res. Lett.,* **38,** L15803, doi:10.1029/2011GL048249.

Fudeyasu, H., Y. Wang, M. Satoh, T. Nasuno, H. Miura, and W. Yanase, 2008: The global cloud-system-resolving model NICAM successfully simulated the lifecycles of two real tropical cyclones. *Geophys. Res. Lett.,* **35,** L22808, doi:10.1029/2008GL036003.

Huffman, G. J., R. F. Adler, B. Rudolf, U. Schneider, and P. R. Keehn, 1995: Global precipitation estimates based on a technique for combining satellite-based estimates, rain gauge analysis, and NWP model precipitation information. *J. Climate,* **8,** 1284–1295, doi:10.1175/1520-0442(1995)008<1284:GPEBOA>2.0.CO;2.

Jia, L., and Coauthors, 2015: Improved seasonal prediction of temperature and precipitation over land in a high-resolution GFDL climate model. *J. Climate,* doi:10.1175/JCLI-D-14-00112.1, in press.

Jiang, X., M. Zhao, and D. E. Waliser, 2012: Modulation of tropical cyclones over the eastern Pacific by the intraseasonal variability simulated in an AGCM. *J. Climate,* **25,** 6524–6538, doi:10.1175/JCLI-D-11-00531.1.

Kerr, R. A., 2012: One Sandy forecast a bigger winner than others. *Science,* **338,** 736–737, doi:10.1126/science.338.6108.736.

Knapp, K. R., M. C. Kruk, D. H. Levinson, H. J. Diamond, and C. J. Neumann, 2010: The International Best Track Archive for Climate Stewardship (IBTrACS). *Bull. Amer. Meteor. Soc.,* **91,** 363–376, doi:10.1175/2009BAMS2755.1.

Lander, M., C. Guard, and S. Camargo, 2014: Super Typhoon Haiyan [in "State of the Climate in 2013"]. *Bull. Amer. Meteor. Soc.,* **95,** S112–S114, doi:10.1175/2014BAMSStateoftheClimate.1.

Landsea, C. W., 1993: A climatology of intense (or major) Atlantic hurricanes. *Mon. Wea. Rev.,* **121,** 1703–1713, doi:10.1175/1520-0493(1993)121<1703:ACOIMA>2.0.CO;2.

Leroy, A., and M. C. Wheeler, 2008: Statistical prediction of weekly tropical cyclone activity in the Southern Hemisphere. *Mon. Wea. Rev.,* **136,** 3637–3654, doi:10.1175/2008MWR2426.1.

Li, T., 2012: Synoptic and climatic aspects of tropical cyclogenesis in Western North Pacific. *Cyclones: Formation, Triggers and Control,* K. Oouchi and H. Fudeyasu, Eds., Nova Science Publishers, Inc., 61–94.

Liebmann, B., H. H. Hendon, and J. D. Glick, 1994: The relationship between tropical cyclones of the western Pacific and Indian Oceans and the Madden-Julian Oscillation. *J. Meteor. Soc. Japan,* **72,** 401–411.

Malakoff, D., 2012: Scientists assess damage from Sandy's deadly punch. *Science,* **338,** 728–729, doi:10.1126/science.338.6108.728.

Maloney, E. D., and D. L. Hartmann, 2000: Modulation of hurricane activity in the Gulf of Mexico by the Madden–Julian oscillation. *Science,* **287,** 2002–2004, doi:10.1126/science.287.5460.2002.

Mo, K. C., 2000: The association between intraseasonal oscillations and tropical storms in the Atlantic basin. *Mon. Wea. Rev.,* **128,** 4097–4107, doi:10.1175/1520-0493(2000)129<4097:TABIOA>2.0.CO;2.

Peng, M. S., B. Fu, T. Li, and D. E. Stevens, 2012: Developing versus nondeveloping disturbances for tropical cyclone formation. Part I: North Atlantic. *Mon. Wea. Rev.,* **140,** 1047–1066, doi:10.1175/2011MWR3617.1.

Putman, W. M., and S.-J. Lin, 2007: Finite-volume transport on various cubed-sphere grids. *J. Comput. Phys.,* **227,** 55–78, doi:10.1016/j.jcp.2007.07.022.

Reynolds, R. W., T. M. Smith, C. Liu, D. B. Chelton, K. S. Casey, and M. G. Schlax, 2007: Daily high-resolution-blended analyses for sea surface temperature. *J. Climate,* **20,** 5473–5496, doi:10.1175/2007JCLI1824.1.

Ritchie, E. A., and G. J. Holland, 1999: Large-scale patterns associated with tropical cyclogenesis in the western Pacific. *Mon. Wea. Rev.,* **127,** 2027–2043, doi:10.1175/1520-0493(1999)127<2027:LSPAWT>2.0.CO;2.

Shaevitz, D. A., and Coauthors, 2014: Characteristics of tropical cyclones in high-resolution models in the present climate. *J. Adv. Model. Earth Syst.,* doi:10.1002/2014MS000372, in press.

Tam, C.-Y., and T. Li, 2006: The origin and dispersion characteristics of the observed tropical summertime synoptic-scale waves over the western Pacific. *Mon. Wea. Rev.,* **134,** 1630–1646, doi:10.1175/MWR3147.1.

Vecchi, G. A., and Coauthors, 2014: On the seasonal forecasting of regional tropical cyclone activity. *J. Climate,* **27,** 7994–8016, doi:10.1175/JCLI-D-14-00158.1.

Vitart, F., 2009: Impact of the Madden–Julian Oscillation on tropical tropical cyclones and risk of landfall in the ECMWF forecast system. *Geophys. Res. Lett.,* **36,** L15802, doi:10.1029/2009GL039089.

——, 2014: Evolution of ECMWF sub-seasonal forecast skill scores. *Quart. J. Roy. Meteor. Soc.*, **140,** 1889–1899, doi:10.1002/qj.2256.

Waliser, D. E., and Coauthors, 2009: MJO simulation diagnostics. *J. Climate,* **22,** 3006–3030, doi:10.1175/2008JCLI2731.1.

Wang, Z., M. T. Montgomery, and T. J. Dunkerton, 2009: A dynamically-based method for forecasting tropical cyclogenesis location in the Atlantic sector using global model products. *Geophys. Res. Lett.,* **36,** L03801, doi:10.1029/2008GL035586.

Yang, X., and Coauthors, 2013: A predictable AMO-like pattern in the GFDL fully coupled ensemble initialization and decadal forecasting system. *J. Climate,* **26,** 650–661, doi:10.1175/JCLI-D-12-00231.1.

Zhang, S., M. Zhao, S. J. Lin, X. Yang, and W. Anderson, 2014: Retrieval of tropical cyclone statistics with a high-resolution coupled model and data. *Geophys. Res. Lett.,* **41,** 652–660, doi:10.1002/2013GL058879.

Zhao, M., I. M. Held, S.-J. Lin, and G. A. Vecchi, 2009: Simulations of global hurricane climatology, interannual variability, and response to global warming using a 50-km resolution GCM. *J. Climate,* **22,** 6653–6678, doi:10.1175/2009JCLI3049.1.